Application Note
AN 20-001

SEMIKRON DANFOSS

Revision:	03
Issue date:	2024-09-19
Prepared by:	Paul Drexhage, Arendt Wintrich
Approved by:	Peter Beckedahl

Keyword: IGBT module, temperature sensor, thermal impedance

Calculating Junction Temperature Using a Module Temperature Sensor

1. Introduction

A legitimate but complex question is: how does one use the integrated temperature sensor inside a power semiconductor module to determine the virtual junction temperature? There are several answers depending on the required accuracy and the goal of the temperature prediction. This application note will explain two possible methods: one at the lower end and one at the higher end of the complexity scale. It is first necessary

to define the goals of the temperature prediction because it has an impact on the required device parameters, qualification effort, and computing power for calculation. This document uses the example of a three-phase 2-level inverter circuit with IGBTs and freewheeling diodes but these methods can be applied to other circuits and semiconductors as well. Though the proposed procedures refer to module-integrated temperature sensors, they can also be used for external sensors (e.g. on the heatsink). The intention is that the calculation methods are implemented using a digital processor on a converter control board.

Table 1: Comparison of the two considered methods for junction temperature prediction

Simplified solution for quasi-steady state conditions	**Complex solution for short high overload and stall torque conditions**
Calculation of losses in one switch and assuming the other switches in a symmetric circuit have equal losses (e.g. IGBT1…6 in a three-phase inverter)	Calculation of the losses for any switch according to actual circuit conditions (V_{CC}, V_{out}, I_{out}, cos(φ), f_{sw}, T_j)
Only one thermal model (T_j to sensor T_r) per type of switch is required (e.g. one for diode, one for IGBT)	Calculation of the junction temperature using a $Z_{th(j-r)}$-matrix including coupling of all relevant switches
Sampling rates on the order of 100ms…1s which allows use of R_{th} instead of Z_{th}	Sampling rate on the order of $1/f_{sw}$ (or multiples of that)
Result: average losses of periodic function and average junction temperatures	**Result:** instantaneous function of losses and device temperatures
Correction factor used to account for temperature ripple due to fundamental output frequency	Temperature swing at inverter output frequency is inherently calculated
"Envelope curve" for temperatures usable for device protection	
Advantage: Low computing power and data volume	**Advantages:** Protection at low frequency or stall torque possible. Information about temperature cycle stress available.
Disadvantages: Limited protection in stall torque or at short high overload. No usable information for temperature cycle stress calculations.	**Disadvantages:** High effort for model implementation. High computing power required. High data volume.

2. Temperature Prediction Goals

2.1 Over temperature protection

The most common use of temperature monitoring is simply to protect the semiconductors from operating above their thermal limits. With gradually increasing junction temperature situations (e.g. increases in ambient temperature or low magnitude/long duration overloads), this can be accomplished by comparing the sensor temperature with a pre-determined (at the design stage) set point at which the system faults (or issues a warning). For dynamic loads, power fold back curves can be developed which maximize the output current at a given temperature (e.g. high current at low ambient temperature).

2.2 Performance optimization

The maximum output power of a system at a given operating point can depend on a variety of factors, among them environmental (ambient air temperature, altitude) as well as electrical (fundamental output frequency). The output current can be maximized for a given operating point while ensuring that the junction temperature does not exceed its limits. However, this approach carries the risk of reducing power module lifetime if the additional temperature stress is not considered (see explanation of power cycling in [2]).

2.3 Lifetime prediction

Most power cycling lifetime models are based primarily on the mean junction temperature and number of junction temperature excursions (sec. 2.7.6 in [2]). In theory, this means that a system that can calculate and store the value of actual junction temperature during operation could actively apply a lifetime model to

determine the "life remaining" in a system. In practice, this has proven difficult to achieve due to the uncertainty of lifetime models coupled with the complexity (and cost) of storing, processing, and evaluating such data in the field.

3. Integrated Temperature Sensors

Modern power semiconductor modules incorporate a temperature-sensitive resistive element (thermistor; NTC or PTC) soldered on the DBC substrate. Due to layout restrictions (e.g. voltage isolation), the temperature (T_r) of this sensor does not represent the actual IGBT or diode junction temperature.

Figure 1: Location of temperature sensors in baseplate-less MiniSKiiP (L) and baseplate SEMiX 3 Press-Fit (R)

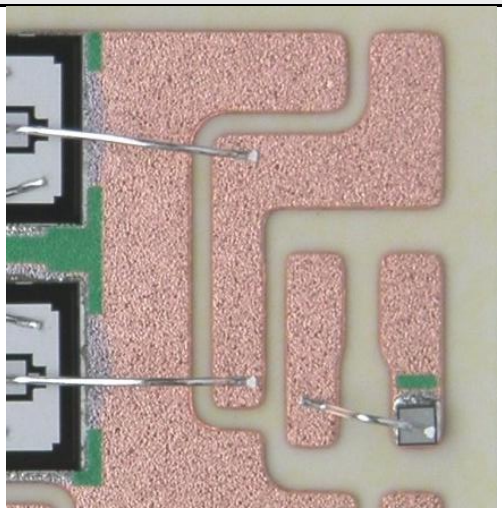

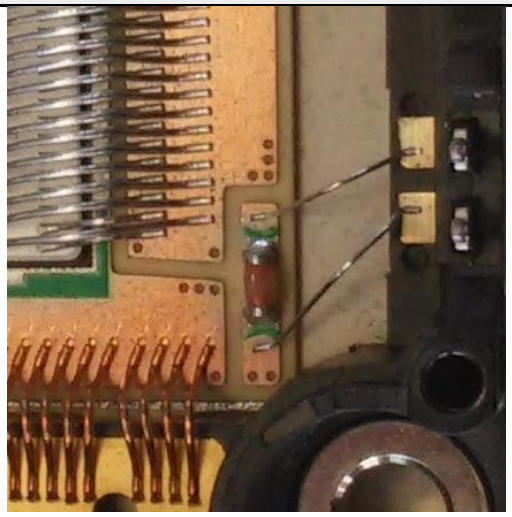

For Semikron Danfoss product, the temperature of the sensor may be specified as approximating an existing reference point (e.g. T_c or T_s). This is specified in the Technical Explanations for the product. For example:

- SEMiX 3s: Sensor is on a separate DBC substrate → T_r is close to T_s
- SKiiP 4: Sensor is on the same copper trace as IGBT and diode → $T_s < T_r < T_j$

However, this simplification should be used with caution as T_r can vary depending on several conditions. In some cases, the sensor temperature may be lower than the heatsink temperature beneath the hottest chip.

The temperature sensor can be treated as a node within a simplified Foster thermal network. If only overtemperature protection for slowly changing loads is required and the sensor temperature is equal to heatsink temperature, then the datasheet values for $R_{th(j-s)}$ can be used with safety margin to estimate junction temperature. For more accurate results under dynamic conditions, a dedicated $Z_{th(j-r)}$ must be determined.

3.1 Why are no $R_{th(j-r)}/Z_{th(j-r)}$ values specified in the module data sheet?

The sensor temperature and resulting thermal impedance from "junction to sensor" depend on many conditions that are outside the design of the module itself. These conditions influence both lateral temperature spreading and vertical heat conductivity in the system and can be divided roughly into two parts.

3.1.1 Influence of heatsink

The mechanical design of the heatsink influences the distribution of heat beneath the module, due in part to:

- Cooling medium (air or liquid)
- Material and root thickness of the heatsink
- Conductivity and thickness of thermal paste layer
- Module and sensor position on heatsink (distance to edges and flow direction of cooling medium, see Figure 2)
- Distance to other modules on the same heatsink

Figure 2: Effect of module mounting position on sensor temperature

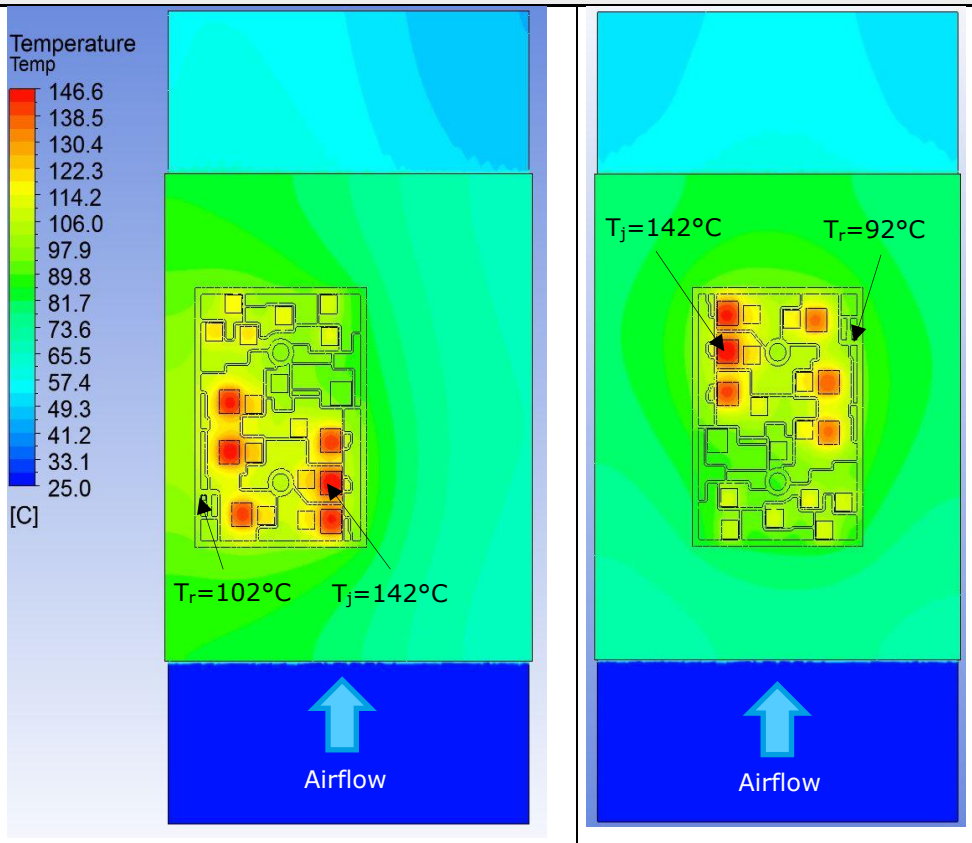

Therefore, power semiconductor modules are specified in their data sheet with $R_{th(j-s)}$ or $R_{th(j-c)}$ and not $R_{th(j-r)}$, except for modules that are qualified and delivered together with a heatsink (SKiiP).

3.1.2 Influence of operating point

The electrical operating point of the system determines the magnitude and distribution of losses between switches within the module.

Figure 3 shows two simulations of a 50A/1200V Converter-Inverter-Brake (CIB) module on an air cooled heatsink (T_a = 25°C, $R_{th(s-a)}$ ≈ 0.13K/W). The left side shows the condition of "inverter" operation (22kW, cos(ϕ) = 0.85) with high load on the IGBT and the DC-link fed by the input rectifier. The right side shows the same module during "brake" operation (22kW, cos(ϕ) = -0.85) with the braking energy dissipated by the brake chopper. The temperature sensor is at the lower left corner.

Figure 3: Top view of a MiniSKiiP 3 CIB module on air-cooled heatsink under two operating conditions: inverting with cos(ϕ) = 0.85 (L) and braking with cos(ϕ) = -0.85 (R)

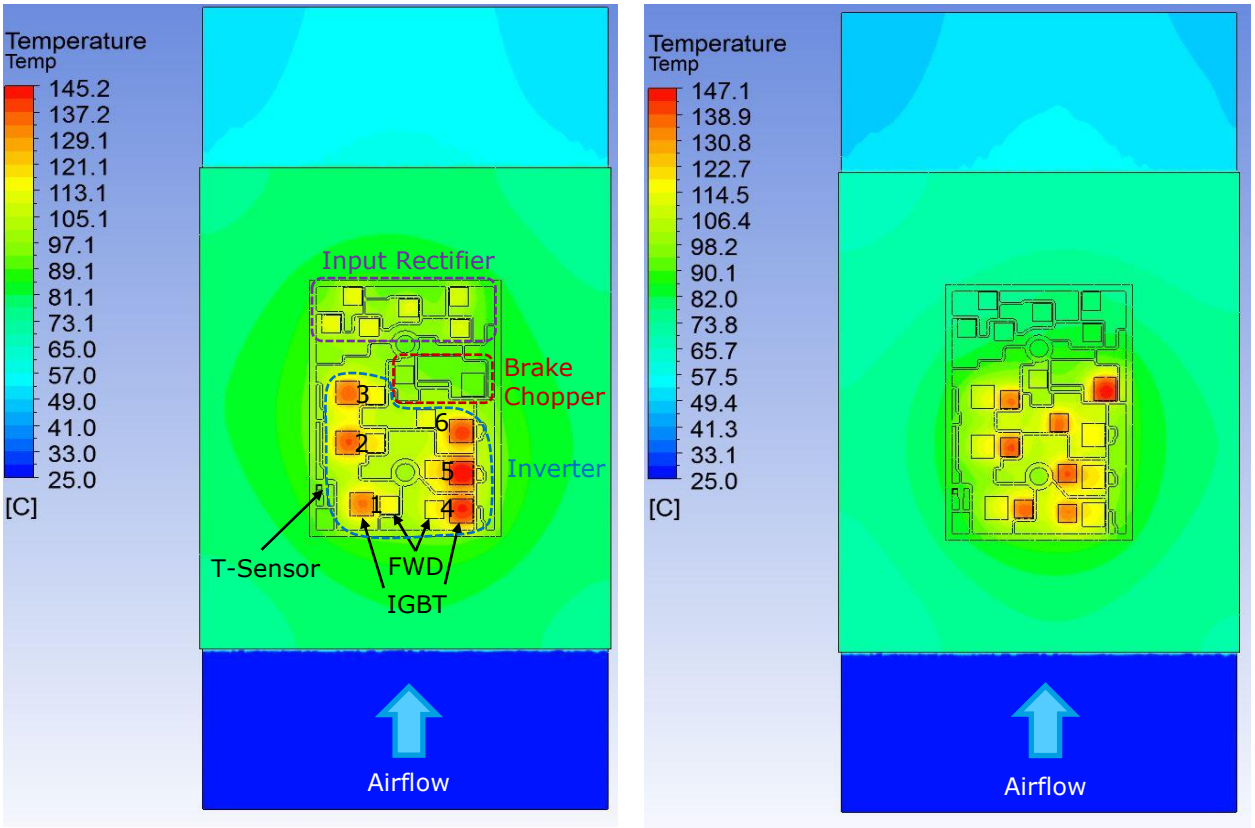

Table 2 indicates that there is a noticeable variation in thermal resistance between two operating conditions.

Table 2: Variation in $R_{th(j-r)}$ between two operating conditions

	Inverting Operation (cos(ϕ) = 0.85)	**Braking Operation (cos(ϕ) = -0.85)**
Calculated $R_{th(j-r)}$: hottest IGBT to sensor	0.81K/W (IGBT5)	0.73K/W (Brake IGBT)
Calculated $R_{th(j-r)}$: hottest inverse diode to sensor	2.25K/W (diode5)	1.18K/W (diode2)
Calculated $R_{th(j-r)}$: hottest rectifier diode to sensor	0.96K/W (diode9)	N/A (No losses)

Furthermore, $R_{th(j-r)}$ can vary considerably from $R_{th(j-s)}$, indicating that the "$T_r \approx T_s$" assumption mentioned earlier has limitations in certain modules. This is shown in Table 3.

Table 3: Effect of "$T_s = T_r$" assumption on calculated temperatures	
	Inverting Operation **(cos(ϕ) = 0.85)** IGBT: 60W Inverse diode: 12W Rectifier diode: 20W
$R_{th(j-r)}$: hottest IGBT to sensor	0.81K/W (IGBT5)
ΔT_{j-r_IGBT}	60W * 0.81K/W = 48.6K
Datasheet $R_{th(j-s)\_IGBT}$	0.71K/W
Calculated ΔT_{j-r} (assumption: $T_r \approx T_s$)	60W * 0.71K/W = 42.6K (*6K too low*)
Calculated $R_{th(j-r)}$: hottest inverse diode to sensor	2.25K/W (diode5)
$\Delta T_{j-r\_inverse\_diode}$	12W * 2.25K/W = 27K
Datasheet $R_{th(j-s)\_diode}$	0.95K/W
Calculated ΔT_{j-r} (assumption: $T_r \approx T_s$)	12W * 0.95K/W = 11.4K (*15.6K too low*)
Calculated $R_{th(j-r)}$: hottest rectifier diode to sensor	0.96K/W (diode9)
$\Delta T_{j-r\_rectifier}$	20W * 0.96K/W = 19.2K
Datasheet $R_{th(j-s)\_rectifier}$	0.9K/W
Calculated ΔT_{j-r} (assumption: $T_r \approx T_s$)	20W * 0.9K/W = 18K (*1.2K too low*)

4. Determining $R_{th(j-r)}/Z_{th(j-r)}$

4.1 Measurement methods

For the reasons listed above, the thermal resistance/impedance from junction to sink must be determined for each application. Three experimental methods can be used to determine the thermal resistance between each individual IGBT or diode switch and the thermal sensor. These results should then be compared with a computer-based finite element model to verify the tests and allow for quicker derivation of thermal resistance under other operating conditions.

In each test, a current is fed through a single switch and the temperatures of the sensor and a target switch are measured (Figure 4).

For $R_{th(j-r)}$, the current is a fixed direct current and the temperature of the sensor measured once stabilized. For $Z_{th(j-r)}$, the current is a step function and the temperature is sensor measured continuously. The current and the voltage across the switch are used to calculate the losses. In practice a step down function is used (turn-off power dissipation) and the measured temperatures are inverted later as this is the only way to reach steady state for temperature dependent losses.

Figure 4: Application of current and resulting temperatures

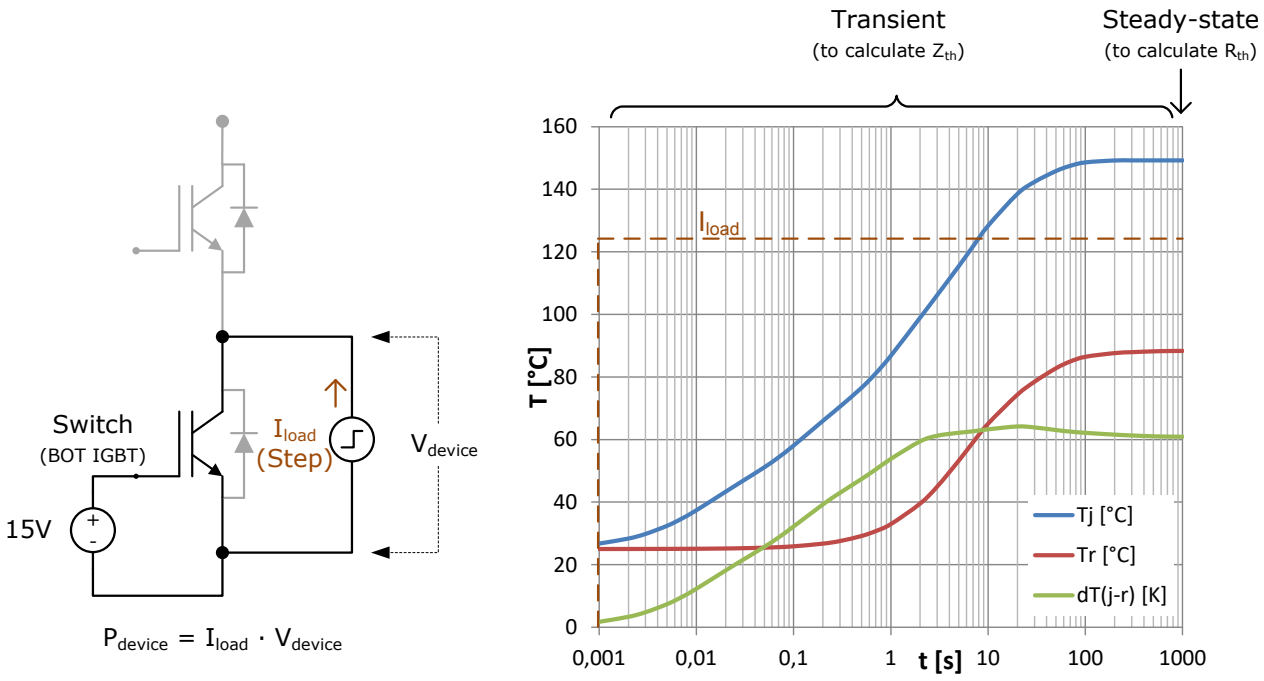

4.1.1 Thermocouple (R_{th})

A specially prepared module is obtained from the manufacturer where thermocouples have been glued to the surface of the chips with thermally conductive epoxy (Figure 5). A regulated direct current (at low voltage) is put through the IGBT or diode and the temperature of the thermocouple and temperature sensor are measured to calculate the temperature difference.

$$R_{th(j-r)} = \frac{T_{j\_device\_thermocouple} - T_r}{P_{device}} \qquad (1)$$

Due to the slow time response of thermocouples, only determination of static thermal resistance $R_{th(j-r)}$ is possible. Furthermore, the thermocouples themselves can introduce 5…15°C of error as the metal wire acts as a heatsink on the top surface of the chip. Caution must be taken to isolate the thermocouples where they connect with measurement equipment.

Figure 5: SEMiX 3 Press-Fit module with thermocouples added to the IGBT chips

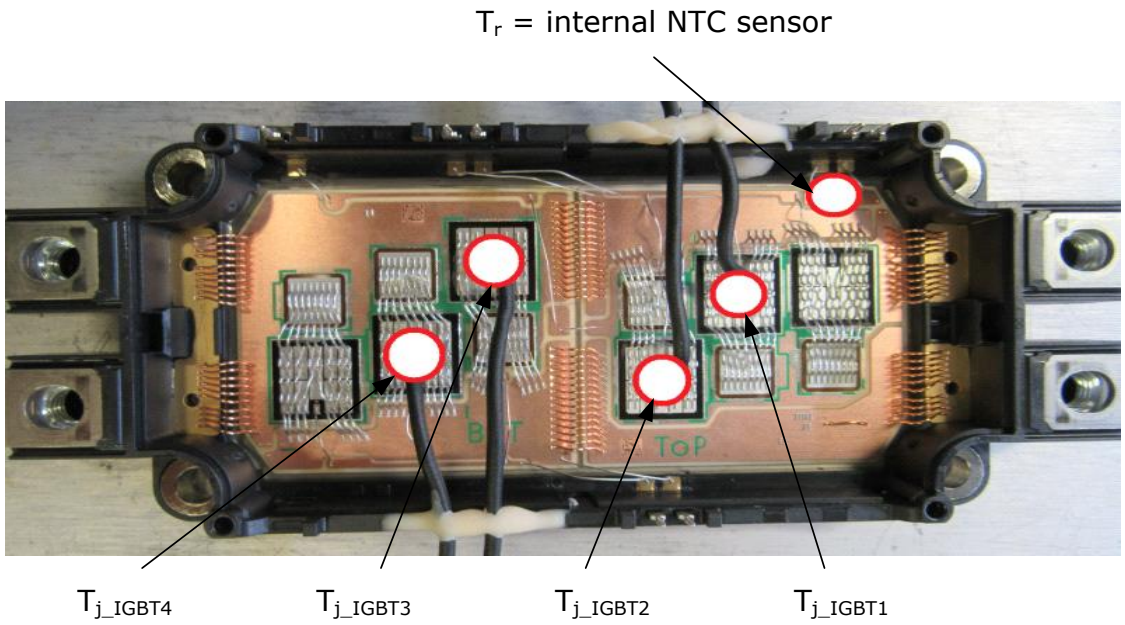

4.1.2 Infrared camera (R_{th})

A specially prepared module without silicone soft mold is used. The housing cover is removed and the interior of the module coated with a matte paint with uniform emissivity to prevent reflections. A regulated direct current (at low voltage) is put through the IGBT or diode and the temperature reported by the camera and the temperature sensor are measured to calculate the temperature difference (Figure 6).

$$R_{th(j-r)} = \frac{T_{j\_device\_IR\_camera} - T_r}{P_{device}} \qquad (2)$$

If properly calibrated a high resolution infrared camera gives accurate temperatures although at a slow enough refresh rate that only determination of static thermal resistance $R_{th(j-r)}$ is possible. Furthermore, modules with internal busbars system cannot be easily measured as the view of the chips is blocked.

Figure 6: SEMiX3p module under infrared imaging

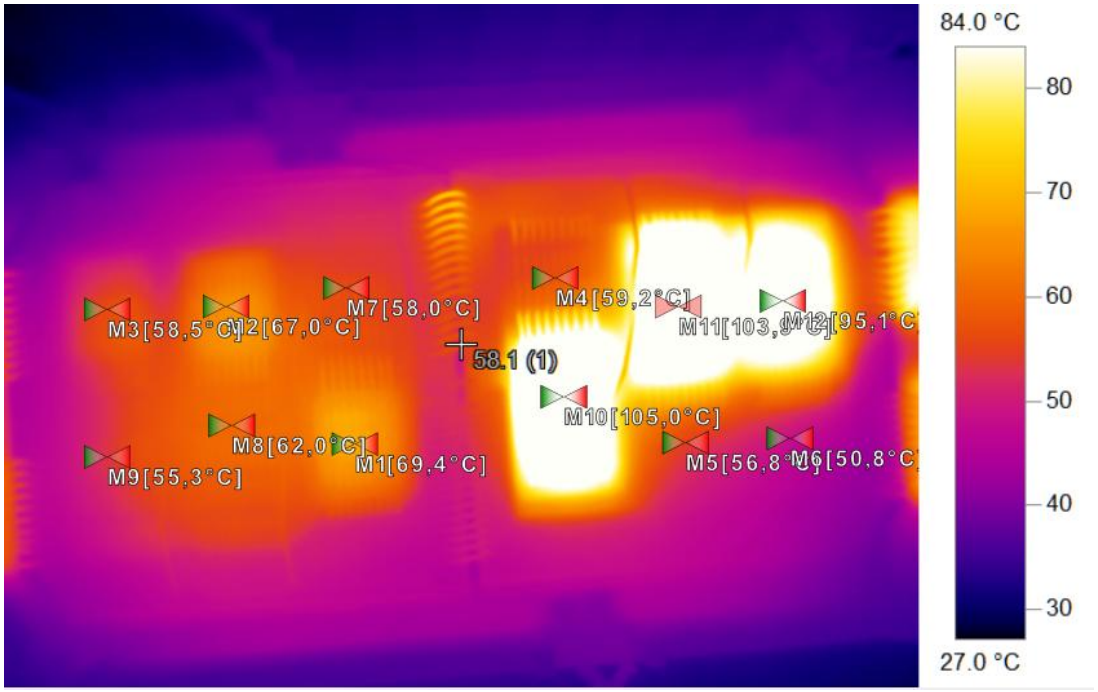

4.1.3 V_{ce} method (R_{th} or Z_{th})

Semiconductors have a linear relationship between junction temperature, T_j, and forward voltage drop, V_{ce}/V_f, at low currents. Using uniform heating in a lab environment, a calibration curve for a particular semiconductor type can be derived (Figure 7). The module is then placed in a fixture where a high current pulse is put through the semiconductor to generate losses and is followed quickly by a low current to measure the forward voltage drop (and hence the junction temperature.)

Figure 7: Test configuration and example calibration curve

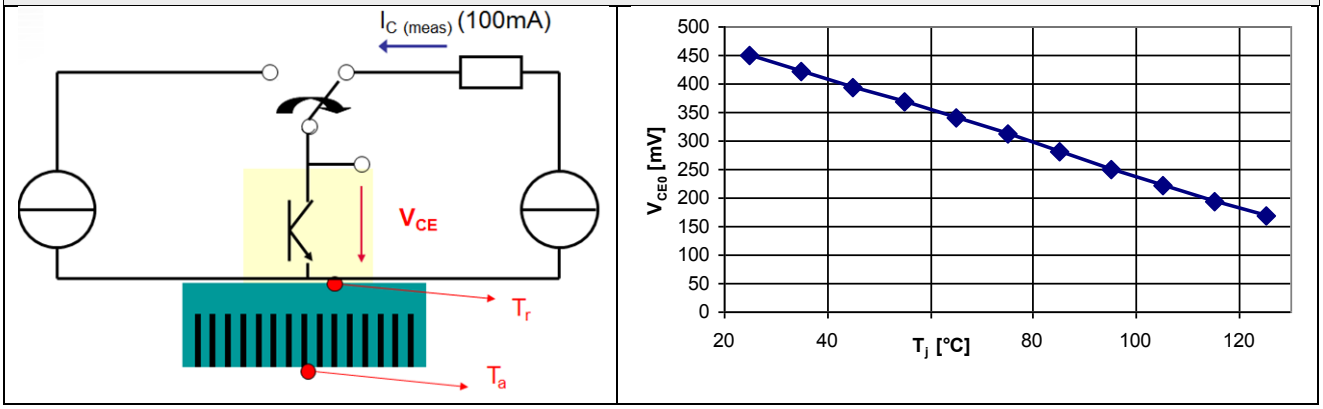

This method provides highly accurate results and can be used to determine the transient thermal impedance (Z_{th}) of the junction-to-sensor interface. However, it usually requires purpose-built test equipment.

4.1.4 Finite Element Analysis (R_{th} or Z_{th})

Finite Element Analysis (FEA) is achieved by modelling the module-heatsink system in software. In order to construct this model, two items are required from the module manufacturer:

- The X-Y locations of the chips within the module ("die map," "chip layout").
- The thickness, density, thermal conductivity, and thermal capacity of the layers making up the module in the Z-axis ("material stack-up").

Once the model is constructed, losses can be applied to each switch and the junction, heatsink, and sensor temperatures determined. This method should be done in conjunction with one of the other test methods to verify the accuracy of the model (and vice versa).

5. Simplified Method for Periodic Functions (Quasi-Steady State Conditions)

An integral solution calculates average losses of the devices over a period (e.g. one fundamental cycle for a PWM inverter). The device losses are the sum of conduction losses, P_{cond}, and switching losses, P_{sw}. The sampling rate is low, for example, in the range of $10/f_{out}$ up to 1s. Therefore, a static thermal resistance, $R_{th(j-r)}$, is used. The losses are temperature-dependent which means an iterative calculation with T_j as an additional input is required. If the losses do not change too much from time step to time step then T_j from the previous time step can be used.

5.1 Required circuit parameters (inverter example)

I_{rms} - Fundamental output current, RMS
M - Modulation depth
cos(φ) - Power factor
V_{cc} - DC link voltage
f_{sw} - Switching (carrier) frequency
f_{out} - Fundamental output frequency

5.2 Loss calculation

Cycle average losses for an IGBT in a three-phase PWM inverter:

$$P_{cond\_IGBT} = \left(\frac{1}{2\pi} + \frac{M \cdot \cos(\varphi)}{8}\right) \cdot \left(V_{CE0\_25°C} + TC_{Vce} \cdot (T_j - 25°C)\right) \cdot I_{pk} + \left(\frac{1}{8} + \frac{M \cdot \cos(\varphi)}{3\pi}\right) \cdot \left(r_{CE\_25°C} + TC_{rce} \cdot (T_j - 25°C)\right) \cdot I_{pk}^2 \quad (3)$$

$$P_{sw\_IGBT} = f_{sw} \cdot E_{on+off} \cdot \frac{1}{2\pi} \cdot \left(\frac{I_{pk}}{I_{ref}}\right)^{K_i} \cdot \left(\frac{V_{cc}}{V_{ref}}\right)^{K_v} \cdot \left(1 + TC_{sw} \cdot (T_j - T_{j_{ref}})\right) \cdot \gamma(K_i) \quad (4)$$

Cycle average losses for a diode in a three-phase PWM inverter:

$$P_{cond\_D} = \left(\frac{1}{2\pi} - \frac{M \cdot \cos(\varphi)}{8}\right) \cdot \left(V_{F0\_25°C} + TC_{Vf} \cdot (T_j - 25°C)\right) \cdot I_{pk} + \left(\frac{1}{8} - \frac{M \cdot \cos(\varphi)}{3\pi}\right) \cdot \left(r_{f\_25°C} + TC_{rf} \cdot (T_j - 25°C)\right) \cdot I_{pk}^2 \quad (5)$$

$$P_{sw\_D} = f_{sw} \cdot E_{rr} \cdot \frac{1}{2\pi} \cdot \left(\frac{I_{pk}}{I_{ref}}\right)^{K_i} \cdot \left(\frac{V_{cc}}{V_{ref}}\right)^{K_v} \cdot \left(1 + TC_{sw}(T_j - T_{j_{ref}})\right) \cdot \gamma(K_i) \quad (6)$$

K_i - Exponent of current dependency (IGBT ≈ 1, FWD ≈ 0.6)
K_v - Exponent of voltage dependency (IGBT ≈ 1.35, FWD ≈ 0.6)
TC_{sw} - Temperature coefficient (IGBT ≈ 0.003, FWD ≈ 0.006)
$\gamma(K_i)$ - Integral $\int_{\varphi}^{\pi+\varphi} \sin^{K_i}(\alpha-\varphi)d\alpha$ (IGBT: γ(1) = 2, FWD: γ(0.6) = 2.3)

Where the following are given in the module datasheet:

$V_{CE0\_25°C}$
$r_{CE\_25°C}$
E_{on+off} (measured at I_{ref}, V_{ref}, T_{jref})
TC_{Vce} (calculated as a linear relationship between $V_{CE0(low\ temp)}$ and $V_{CE0(high\ temp)}$)
TC_{rce} (calculated as a linear relationship between $r_{CE(low\ temp)}$ and $r_{CE(high\ temp)}$)

$V_{F0\_25°C}$
$R_{F\_25°C}$
E_{rr} (measured at I_{ref}, V_{ref}, T_{jref})
TC_{Vf} (calculated as a linear relationship between $V_{F0(low\ temp)}$ and $V_{F0(high\ temp)}$)
TC_{rf} (calculated as a linear relationship between $r_{f(low\ temp)}$ and $r_{f(high\ temp)}$)

See also [2].

5.3 Junction temperature calculation

This "simplified" method relies on a single static thermal resistance measurement for each type of switch and does not consider the coupling effects between switches. Therefore:

1. The tested switch of each type (IGBT or diode) should be closest (best coupled) to the sensor
2. This approach is only valid for "balanced" losses (e.g. 3 phase inverter where all six IGBTs (or all six diodes) are presumed to have similar losses)
    a. This approach is likely not suitable for stall conditions (e.g. where the half-bridge is operating as a buck converter and the lower IGBT is not close to the temperature sensor)

The standard Foster thermal network is used with thermal resistances referenced to the measured sensor temperature, T_r, at a given time step (Figure 8).

Figure 8: Thermal network referenced to temperature sensor

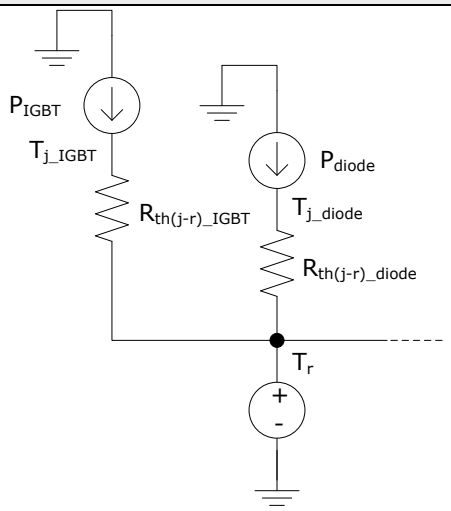

$$T_{j\_IGBT(avg)} = R_{th(j-r)\_IGBT} \cdot P_{IGBT} + T_r \qquad (7)$$

$$T_{j\_diode(avg)} = R_{th(j-r)\_diode} \cdot P_{diode} + T_r \qquad (8)$$

Junction temperature calculation during a single time step (sample) is an iterative process because many chip parameters are temperature dependent.

Figure 9: Calculation process during a single time step

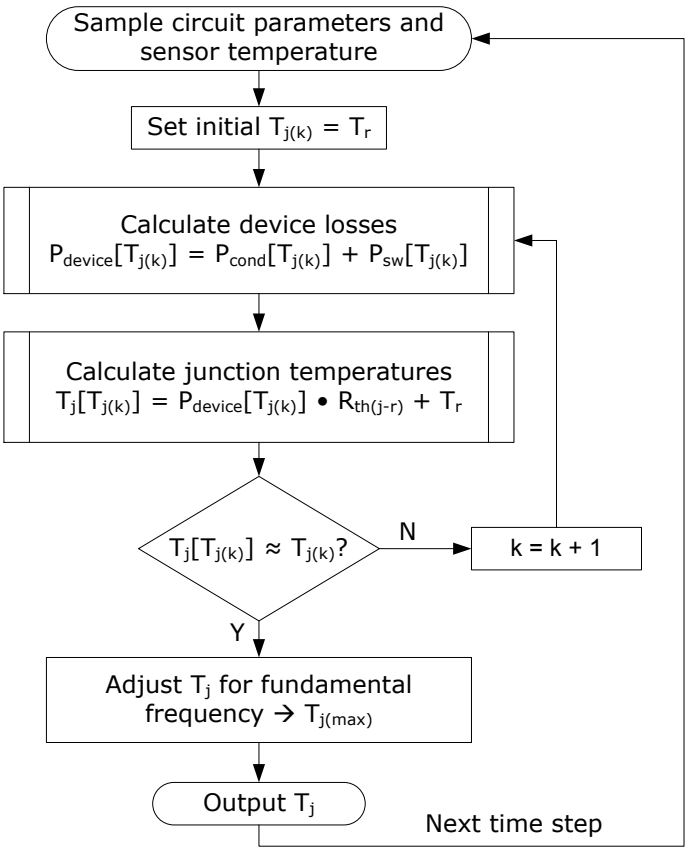

5.4 Correction factor for low output frequencies

The method above yields an average junction temperature and does not indicate the peak temperatures that occur as the junction temperature oscillates at the fundamental output frequency. This is mainly of concern at low (<10Hz) frequency operation. A simple correction factor (as shown in Figure 10) is used to adjust the calculated average temperature. The correction factor depends on the thermal impedance of the devices in use.

Figure 10: Correction factor for $T_{j(max)} = f(f_{out})$

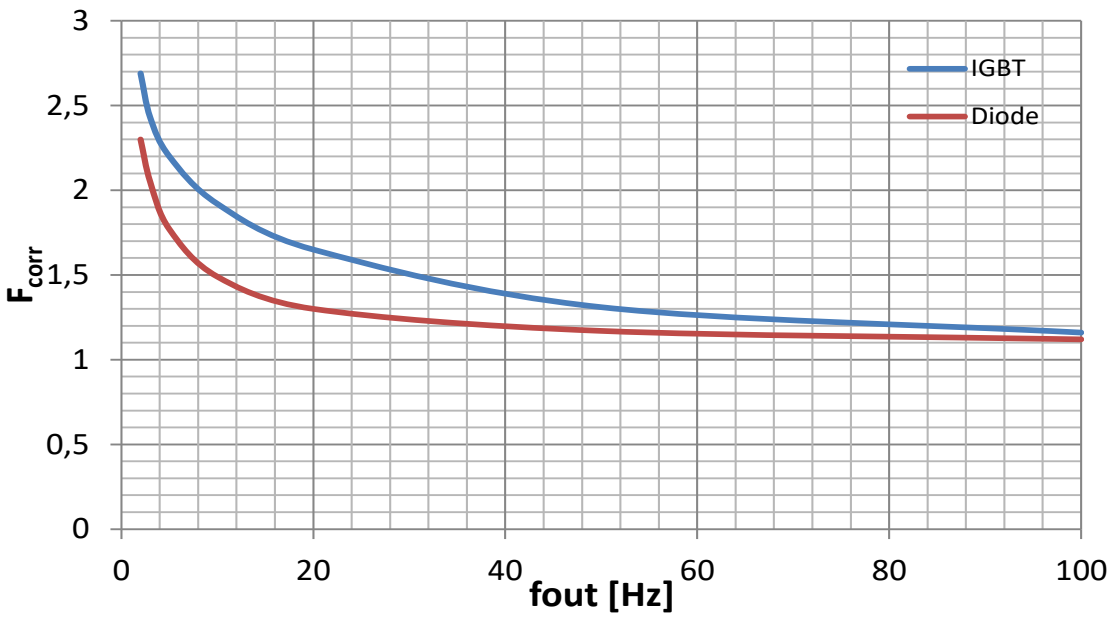

Therefore, the maximum junction temperature during a fundamental cycle can be estimated as:

$$T_{j\_IGBT(max)} = F_{corr\_IGBT} \cdot R_{th(j-r)\_IGBT} \cdot P_{IGBT} + T_r \qquad (9)$$

$$T_{j\_diode(max)} = F_{corr\_diode} \cdot R_{th(j-r)\_diode} \cdot P_{diode} + T_r \qquad (10)$$

5.5 Example (Three-phase PWM inverter)

Device parameters from SKiiP 39AC12T4V1 datasheet:
IGBT: $V_{CE0\_25°C}$=0.8V, $r_{ce\_25°C}$=7mΩ, E_{sw}=36.5mJ, TC_{Vce} = -0.0008V/K, TC_{rce} = 2.67E-5Ω/K
Diode: $V_{F0\_25°C}$=1.3V, $r_{f\_25°C}$=5.6mΩ, E_{rr}=11.4mJ, TC_{Vf} = -0.0032V/K, TC_{rf} = 1.76E-5Ω/K

Measured $R_{th(j-r)}$ from testing:
$R_{th(j-r)I}$ = 0.3 K/W
$R_{th(j-r)D}$ =0.6 K/W

Initial time step: measured values during operation
I_{out} = 76A_{rms} = 107.48Apk
M = 1
cos(φ) = 0.85
V_{CC} = 650V
f_{sw} = 4kHz
f_{out} = 20Hz
T_r = 100°C

Calculated losses
(First iteration shown)

$$P_{cond\_IGBT} = \left(\frac{1}{2\pi} + \frac{1 \cdot 0.85}{8}\right) \cdot \left(0.8V - 0.0008V/K \cdot (100°C - 25°C)\right) \cdot 107.48A + \left(\frac{1}{8} + \frac{1 \cdot 0.85}{3\pi}\right) \cdot \left(0.007\Omega + 0.0000267\Omega/K \cdot (100°C - 25°C)\right) \cdot 107.48A^2 = 43.49W$$

$$P_{sw\_IGBT} = 4000Hz \cdot 0.0365J \cdot \frac{1}{2\pi} \cdot \left(\frac{107.48A}{150A}\right)^1 \cdot \left(\frac{650V}{600V}\right)^{1.35} \cdot \left(1 + 0.003 \cdot (100°C - 150°C)\right) \cdot 2 = 31.53W$$

$$P_{cond\_D} = \left(\frac{1}{2\pi} - \frac{1 \cdot 0.85}{8}\right) \cdot (1.3V - 0.0032V/K \cdot (100°C - 25°C)) \cdot 107.48A + \left(\frac{1}{8} - \frac{1 \cdot 0.85}{3\pi}\right) \cdot (0.0056\Omega + 0.0000176\Omega/K \cdot (100°C - 25°C)) \cdot 107.48A^2 = 8.81W$$

$$P_{sw\_D} = 4000Hz \cdot 0.0114J \cdot \frac{1}{2\pi} \cdot \left(\frac{107.48A}{150A}\right)^{0.6} \cdot \left(\frac{650V}{600V}\right)^{0.6} \cdot (1 + 0.006 \cdot (100°C - 150°C)) \cdot 2.3 = 10.04W$$

$$T_{j(avg)\_IGBT} = (43.49W + 31.53W) \cdot 0.3K/W + 100°C = 122.5°C$$

$$T_{j(avg)\_D} = (8.81W + 10.04W) \cdot 0.6K/W + 100°C = 111.3°C$$

Table 4: Example showing stabilization of temperature after two iterations

K	P_{cond_IGBT}	P_{sw_IGBT}	P_{cond_D}	P_{sw_D}	$T_{j(avg)\_IGBT}$	$T_{j(avg)\_D}$
0	-	-	-	-	100°C	100°C
1	43.49W	31.53W	8.81W	10.04W	123°C	111°C
2	44.47W	34.04W	8.68W	11.01W	124°C	112°C
3	44.51W	34.16W	8.68W	11.05W	124°C	112°C
4	44.52W	34.16W	8.68W	11.06W	124°C	112°C
$T_{j(max)\_IGBT} = 1.65 \cdot (44.52W + 34.16W) \cdot 0.3K/W + 100°C = 139°C$ $T_{j(max)\_D} = 1.3 \cdot (8.68W + 11.06W) \cdot 0.6K/W + 100°C = 115°C$						

6. Thermal Coupling

In operation, the heat generated by adjacent switches affects the temperature of the examined switch, and hence the effective thermal impedance between junction and temperature sensor (Figure 11). These thermal impedances between chips must be quantified to use the "Complex Method" of junction temperature calculation described below.

Figure 11: FEA model of half-bridge module illustrating thermal coupling between chips and temperature sensor

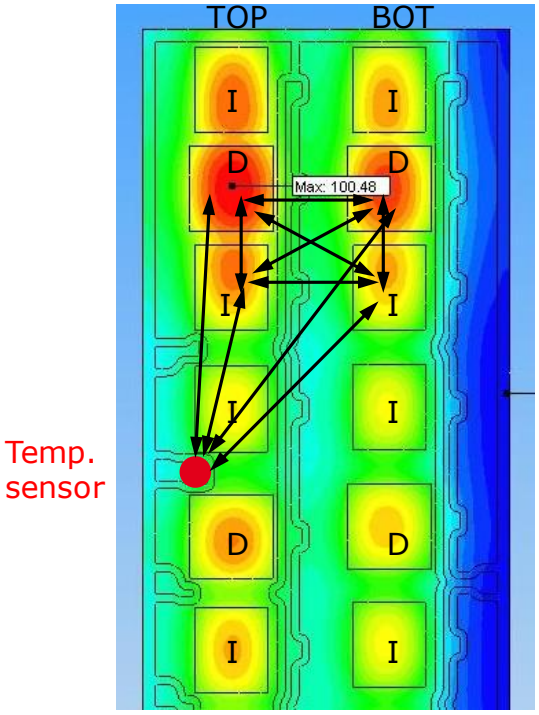

The relationship between any one switch and the temperature sensor is thus defined by the effect the losses in the other switches have on the switch in question (Figure 12). The switch for which you are trying to determine the ultimate junction temperature in the application is referred to as the "Self" switch. Note that in this document the definition of "switch" pertains to a single electrical element (e.g. IGBT or diode) as opposed to other documents that refer to a single switch as being composed of an IGBT and diode.

Figure 12: Definition of static coupling for one switch in a hypothetical half-bridge

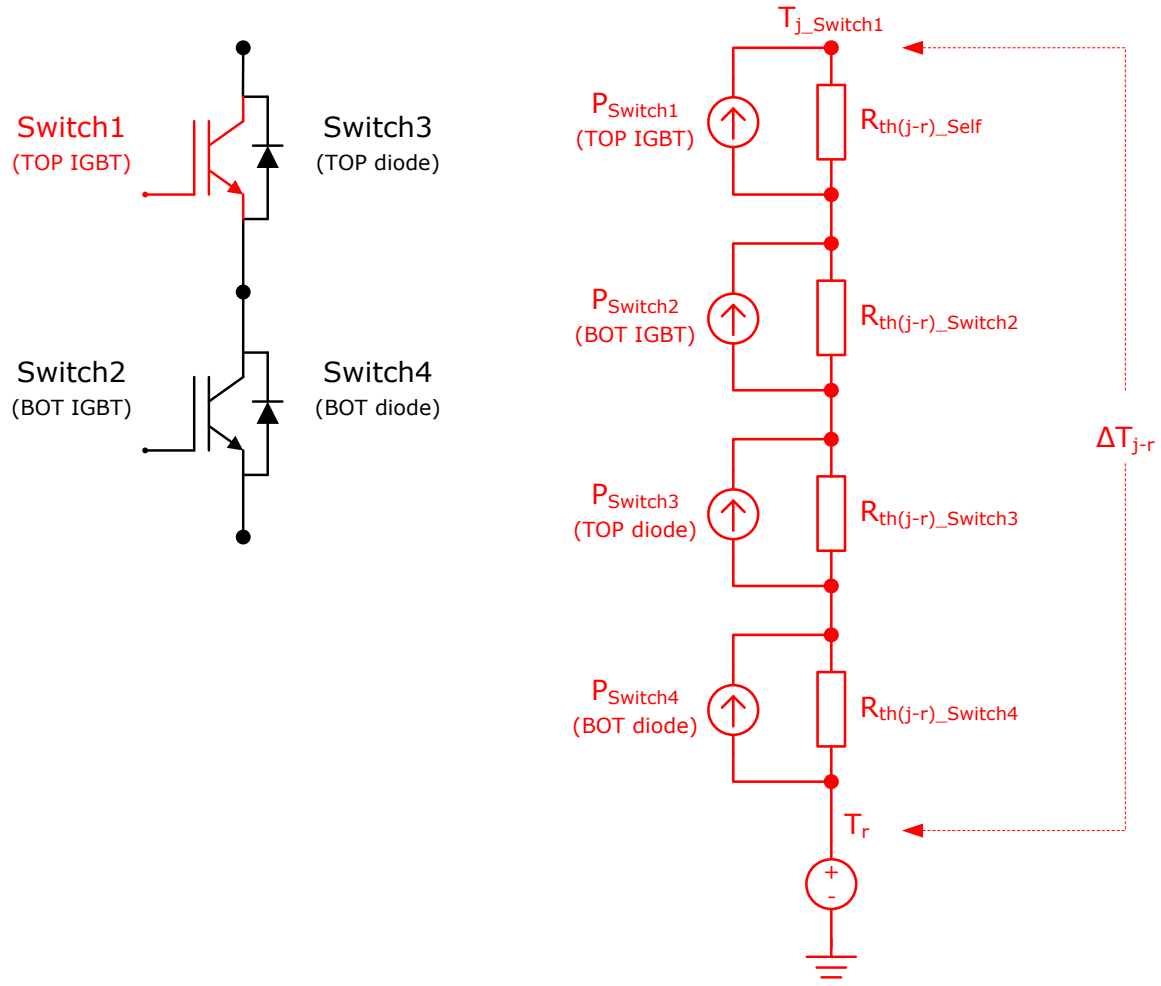

$$T_{j\_Switch1} = T_r + P_{Switch1} \cdot R_{th(j-r)\_Self} + P_{Switch2} \cdot R_{th(j-r)\_Switch2} + P_{Switch3} \cdot R_{th(j-r)\_Switch3} + P_{Switch4} \cdot R_{th(j-r)\_Switch4} \quad (11)$$

6.1.1 Determination of R_{th}/Z_{th} matrix

In a lab setting, losses must be applied to each switch individually and the junction temperature measured using one of the methods in section 4.1. The following example uses the half-bridge circuit from Figure 12.

A. Apply target losses to Switch1 (Self) only. Measure $T_{j\_Switch1}$ and T_r.
Calculate:

$$R_{th(j-r)\_Self} = \frac{T_{j\_Switch1\_A} - T_{r\_A}}{P_{Switch1}} \quad (12)$$

B. Apply target losses to Switch2 only. Measure $T_{j\_Switch1}$ and T_r.
Calculate:

$$R_{th(j-r)\_Switch2} = \frac{T_{j\_Switch1\_B} - T_{r\_B}}{P_{Switch2}} \quad (13)$$

C. Apply target losses to Switch3 only. Measure $T_{j\_Switch1}$ and T_r.
Calculate:

$$R_{th(j-r)\_Switch3} = \frac{T_{j\_Switch1\_C} - T_{r\_C}}{P_{Switch3}} \quad (14)$$

D. Apply target losses to Switch4 only. Measure $T_{j\_Switch1}$ and T_r. Calculate:

$$R_{th(j-r)\_Switch4} = \frac{T_{j\_Switch1\_D} - T_{r\_D}}{P_{Switch4}} \qquad (15)$$

Repeat steps A through D for the remaining three switches. The resulting values can be placed in a matrix as shown in Table 5.

Table 5: Rth matrix for hypothetical half-bridge

Apply losses at: / Measure T_j at:	TOP IGBT (Switch1)	BOT IGBT (Switch2)	TOP Diode (Switch3)	BOT Diode (Switch4)
TOP IGBT (Switch1)	$R_{th(j-r)\_Switch1,1}$ (Self)	$R_{th(j-r)\_Switch1,2}$	$R_{th(j-r)\_Switch1,3}$	$R_{th(j-r)\_Switch1,4}$
BOT IGBT (Switch2)	$R_{th(j-r)\_Switch2,1}$	$R_{th(j-r)\_Switch2,2}$ (Self)	$R_{th(j-r)\_Switch2,3}$	$R_{th(j-r)\_Switch2,4}$
TOP Diode (Switch3)	$R_{th(j-r)\_Switch3,1}$	$R_{th(j-r)\_Switch3,2}$	$R_{th(j-r)\_Switch3,3}$ (Self)	$R_{th(j-r)\_Switch3,4}$
BOT Diode (Switch4)	$R_{th(j-r)\_Switch4,1}$	$R_{th(j-r)\_Switch4,2}$	$R_{th(j-r)\_Switch4,3}$	$R_{th(j-r)\_Switch4,4}$ (Self)

In the case of transient thermal impedance, the term $R_{th(j-r)\_Switch\#,c}$ is replaced by the Foster model elements, $Z_{th(j-r)\_Switch\#,c}$. It should be noted that it is often possible to simplify the matrix if, for example, no thermal coupling between switches is present (zero entries) or if the step response can be modeled by one R_{th}/Tau element only.

7. Complex Method, Step-by-Step (Short, High Overload and Stall Torque Conditions)

During system operation, the losses for any switch are calculated instantaneously using measured values. The sampling rate is high: for example $1/f_{sw}$ or some multiple thereof. If f_{sw} is high compared to f_{out} and the current does not change much during several periods of f_{sw} then it is possible to combine several periods into one calculation step to lower the computing effort.

Prior to system implementation a Z_{th} matrix must be created as described previously. During calculation, this may be simplified to an R_{th} matrix if the sampling rate > 0.5s.

7.1 Required circuit parameters (inverter example)

i(t) - actual value output current
v(t) - actual value of output voltage (line-to-neutral)
M - modulation depth to calculate the actual duty cycle
V_{cc} - DC link voltage
f_{sw} - switching (carrier) frequency

7.2 Loss calculation

Loss calculations are based on a step-down DC/DC ("buck") converter with instantaneous values. For variable definition, see 5.2.

$$DC_{IGBT} = 0.5 + \frac{v(t)}{V_{cc}} \qquad (16)$$

$$DC_{diode} = 1 - DC_{IGBT} \qquad (17)$$

$$P_{cond\_IGBT} = DC_{IGBT} \cdot \left[i(t) \cdot \left(V_{CE0_{25°C}} + TC_{Vce} \cdot (T_j - 25°C) \right) + i(t)^2 \cdot \left(r_{CE\_25°C} + TC_{rce} \cdot (T_j - 25°C) \right) \right] \qquad (18)$$

$$P_{sw\_IGBT} = f_{sw} \cdot E_{on+off} \cdot \left(\frac{|i(t)|}{I_{ref}}\right)^{K_i} \cdot \left(\frac{V_{cc}}{V_{ref}}\right)^{K_v} \cdot \left(1 + TC_{sw} \cdot (T_j - T_{j_{ref}})\right) \quad (19)$$

$$P_{cond\_diode} = DC_{diode} \cdot \left[i(t) \cdot \left(V_{F0\_25°C} + TC_{Vf} \cdot (T_j - 25°C)\right) + i(t)^2 \cdot \left(r_{f\_25°C} + TC_{rf} \cdot (T_j - 25°C)\right)\right] \quad (20)$$

$$P_{sw\_D} = f_{sw} \cdot E_{rr} \cdot \left(\frac{|i(t)|}{I_{ref}}\right)^{K_i} \cdot \left(\frac{V_{cc}}{V_{ref}}\right)^{K_v} \cdot \left(1 + TC_{sw}(T_j - T_{j_{ref}})\right) \quad (21)$$

7.3 Junction temperature calculation

Temperature for any one of the N switches in a module can be calculated at a moment, t_{m+1}, as follows:

$$T_{j\_Switch\#}(t_{m+1}) = T_r(t_m) + \sum_{c=1}^{N} \sum_{i=1}^{n} \left[\Delta T_{j\_Switch\#,c,i}(t_m) \cdot e^{\frac{-\Delta t_m}{\tau_{Switch\#,c,i}}} + R_{th\_Switch\#,c,i} \cdot P_{Switch\#,c}(t_{m+1}) \cdot \left(1 - e^{\frac{-\Delta t_m}{\tau_{Switch\#,c,i}}}\right)\right] \quad (22)$$

Where:

Switch#: switch under investigation (also row index)
c: column index of switch under investigation
N: total number of switches/rows/columns
i: index of Foster element
n: total number of Foster elements for switch under investigation

For a fixed Δt_m, e^{-X} and $(1-e^{-X})$ become a set of constants that can be included in the Z_{th} matrix.

Figure 13: Calculation process per time step

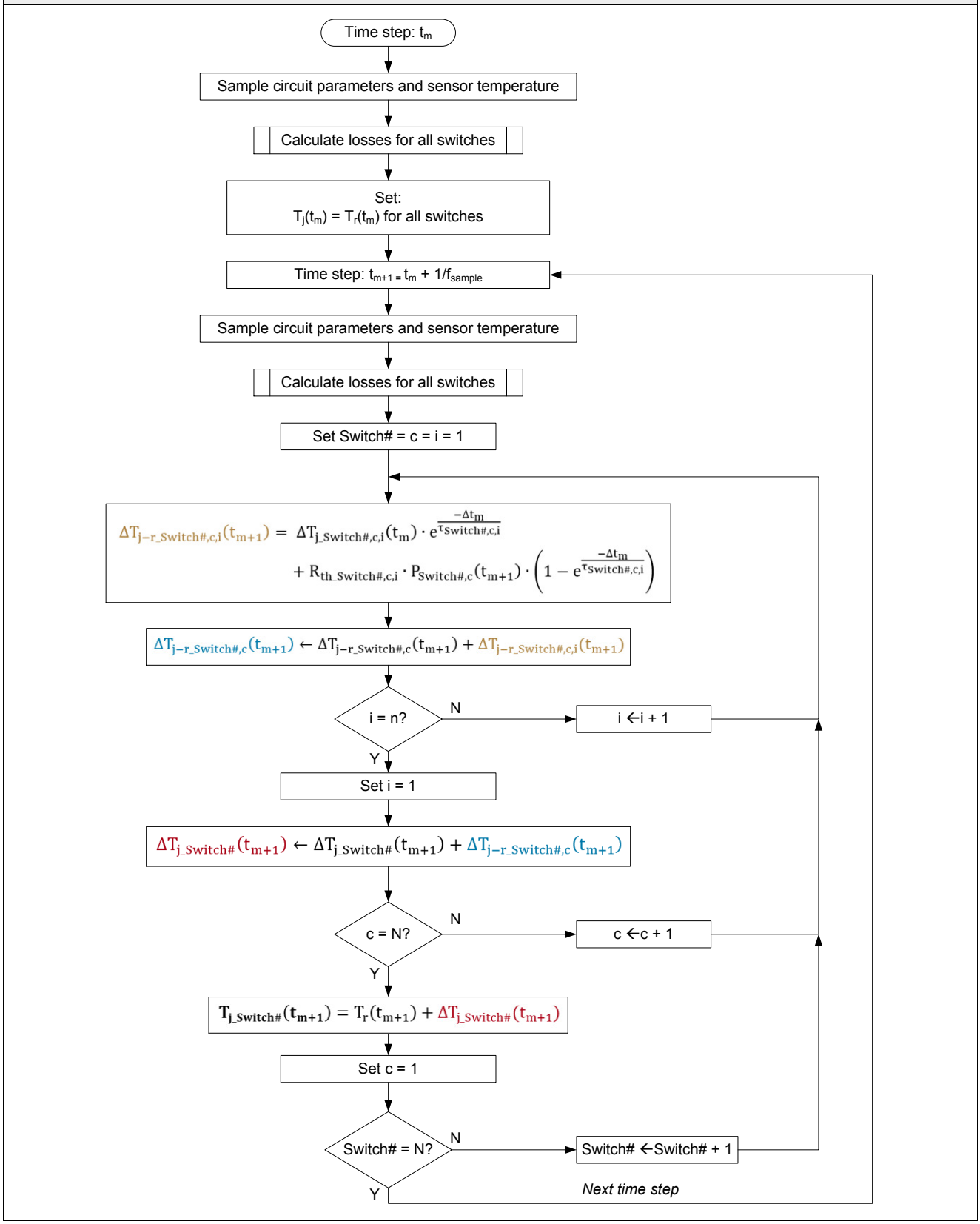

7.4 Example

In the following example, the temperature in the TOP switch of a half-bridge module is calculated using the losses (Table 7) for a theoretical system operating over 1s. Constant losses and a constant temperature

sensor are used for simplicity but the approach is valid for varying values as well. Temperatures at subsequent time steps can be derived using the results from the preceding time step.

Table 6: Example Z_{th} matrix for SEMiX 603GB12E4p on watercooler

c / Switch#	IGBT TOP	IGBT BOT	Diode TOP	Diode BOT
IGBT TOP	i / $R_{th(j-r)}$ / Tau 1 / 0.0054 / 0.0028 2 / 0.0086 / 0.025 3 / 0.0190 / 0.1 4 / 0.0224 / 0.5	i / $R_{th(j-r)}$ / Tau 1 / 0.0063 / 3.7000 2 / 0 / 1 3 / 0 / 1 4 / 0 / 1	i / $R_{th(j-r)}$ / Tau 1 / 0.0248 / 1.2 2 / 0.0024 / 3 3 / 0 / 1 4 / 0 / 1	i / $R_{th(j-r)}$ / Tau 1 / 0.0087 / 4.7 2 / 0 / 1 3 / 0 / 1 4 / 0 / 1
IGBT BOT	$Z_{th(j-r)\_IGBT\_BOT:IGBT\_TOP}$	$Z_{th(j-r)\_IGBT\_BOT:Self}$	$Z_{th(j-r)\_IGBT\_BOT:Diode\_TOP}$	$Z_{th(j-r)\_IGBT\_BOT:Diode\_BOT}$
Diode TOP	$Z_{th(j-r)\_Diode\_TOP:IGBT\_TOP}$	$Z_{th(j-r)\_Diode\_TOP:IGBT\_BOT}$	$Z_{th(j-r)\_Diode\_TOP:Self}$	$Z_{th(j-r)\_Diode\_TOP:Diode\_BOT}$
Diode BOT	$Z_{th(j-r)\_Diode\_BOT:IGBT\_TOP}$	$Z_{th(j-r)\_Diode\_BOT:IGBT\_BOT}$	$Z_{th(j-r)\_Diode\_BOT:Diode\_TOP}$	$Z_{th(j-r)\_Diode\_BOT-Self}$

Table 7: Example run-time parameters used for calculating junction temperature

Time step	**0.0s**	**1.0s**
P_{IGBT_TOP}	300W	300W
P_{IGBT_BOT}	300W	300W
P_{Diode_TOP}	100W	100W
P_{Diode_BOT}	100W	100W
T_{sensor}	80°C	80°C
$T_{j\_IGBT\_TOP}$	80°C	$T_{j\_IGBT\_TOP}(1s)$

$$T_{j\_IGBT\_TOP}(1s) = 80°C + \left[0 \cdot e^{\frac{-1s}{0.0028s}} + 0.0054K/W \cdot 300W \cdot \left(1 - e^{\frac{-1s}{0.0028s}}\right)\right]$$
$$+ \left[0 \cdot e^{\frac{-1s}{0.025s}} + 0.0086K/W \cdot 300W \cdot \left(1 - e^{\frac{-1s}{0.025s}}\right)\right] + \left[0 \cdot e^{\frac{-1s}{0.1s}} + 0.019K/W \cdot 300W \cdot \left(1 - e^{\frac{-1s}{0.1s}}\right)\right]$$
$$+ \left[0 \cdot e^{\frac{-1s}{0.5s}} + 0.0224K/W \cdot 300W \cdot \left(1 - e^{\frac{-1s}{0.5s}}\right)\right] + \left[0 \cdot e^{\frac{-1s}{3.7s}} + 0.0063K/W \cdot 300W \cdot \left(1 - e^{\frac{-1s}{3.7s}}\right)\right]$$
$$+ \left[0 \cdot e^{\frac{-1s}{1.2s}} + 0.0248K/W \cdot 100W \cdot \left(1 - e^{\frac{-1s}{1.2s}}\right)\right] + \left[0 \cdot e^{\frac{-1s}{3s}} + 0.0024K/W \cdot 100W \cdot \left(1 - e^{\frac{-1s}{3s}}\right)\right]$$
$$+ \left[0 \cdot e^{\frac{-1s}{4.7s}} + 0.0087K/W \cdot 100W \cdot \left(1 - e^{\frac{-1s}{4.7s}}\right)\right] = 97.8°C$$

In the example, the TOP IGBT has increased in temperature by 17.8°C after 1s of operation. Of this temperature rise, 15.7°C was due to self-heating of the switch (red terms) and 2.08°C is contributed by the remaining three switches (blue, green, violet terms). In this case, the terms are positive but it could be that terms are negative if the losses in another switch reduce the temperature difference between the sensor and the investigated switch.

8. Summary

Using the integrated temperature sensor to calculate T_j is possible but the accuracy depends on the level of characterization that the designer can undertake during the design process. The most basic protection can be achieved by taking a high safety margin and initiating an overtemperature fault when the sensor reaches a fixed temperature.

A more advanced "simplified" approach involves measuring a thermal impedance $R_{th(j-r)}$ and assuming even loss distribution amongst the switches with average losses for periodic functions. This method requires little computing power and can provide effective temperature protection for converters with well-characterized operation and slow-moving transient overloads.

For protection against fast overloads and special conditions such a "0Hz" inverter operation, a detailed thermal model defining transient thermal impedances between the chips and temperature sensor is required. With careful measurements, individual models can be created for each switch that defines a transient thermal impedance matrix for the entire module. Coupled with strong processing power, this matrix yields a large amount of runtime temperature data that can be used for dynamic protection.

In all cases, it is important to understand that temperature measurement method is only valid for a particular converter design.

References

[1] www.semikron-danfoss.com
[2] A. Wintrich, U. Nicolai, W. Tursky, T. Reimann, "Application Manual Power Semiconductors", 2nd edition, ISLE Verlag 2015, ISBN 978-3-938843-83-3

IMPORTANT INFORMATION AND WARNINGS

The information provided in this document may not be considered as any guarantee or assurance of product characteristics ("Beschaffenheitsgarantie"). This document describes only the usual characteristics of Semikron Danfoss products to be expected in typical applications, which may still vary depending on the specific application. Therefore, products must be tested for the respective application in advance. Resulting from this, application adjustments of any kind may be necessary. Any user of Semikron Danfoss products is responsible for the safety of their applications embedding Semikron Danfoss products and must take adequate safety measures to prevent the applications from causing any physical injury, fire or other problem, also if any Semikron Danfoss product becomes faulty. Any user is responsible for making sure that the application design and realization are compliant with all laws, regulations, norms and standards applicable to the scope of application. Unless otherwise explicitly approved by Semikron Danfoss in a written document signed by authorized representatives of Semikron Danfoss, Semikron Danfoss products may not be used in any applications where a failure of the product or any consequences of the use thereof can reasonably be expected to result in personal injury.
No representation or warranty is given and no liability is assumed with respect to the accuracy, completeness and/or use of any information herein, including without limitation, warranties of non-infringement of intellectual property rights of any third party. Semikron Danfoss does not convey any license under its or a third party's patent rights, copyrights, trade secrets or other intellectual property rights, neither does it make any representation or warranty of non-infringement of intellectual property rights of any third party which may arise from a user's applications. This document supersedes and replaces all previous Semikron Danfoss information of comparable content and scope. Semikron Danfoss may update and/or revise this document at any time.

Semikron Danfoss International GmbH
Sigmundstrasse 200, 90431 Nuremberg, Germany
Tel: +49 911 65596663
sales@semikron-danfoss.com, www.semikron-danfoss.com